HHS Public Access

Author manuscript

*Dev Dyn*. Author manuscript; available in PMC 2018 December 01.

Published in final edited form as:

*Dev Dyn*. 2017 December ; 246(12): 1001–1014. doi:10.1002/dvdy.24598.

# Yolk Sac Erythromyeloid Progenitors Expressing Gain Of Function PTPN11 Have Functional Features Of JMML But Are Not Sufficient To Cause Disease In Mice

**Stefan P. Tarnawsky**[1], **Momoko Yoshimoto**[1,4], **Lisa Deng**[2], **Rebecca J. Chan**[2,3], and **Mervin C. Yoder**[1,3]

[1]Department of Biochemistry and Molecular Biology, Indiana University School of Medicine, Indianapolis, IN 46202, USA

[2]Department of Medical and Molecular Genetics, Indiana University School of Medicine, Indianapolis, IN 46202, USA

[3]Department of Pediatrics, Herman B. Wells Center for Pediatric Research, Indiana University School of Medicine, Indianapolis, IN 46202, USA

## Abstract

**Background—**Accumulating evidence suggests the origin of Juvenile Myelomonocytic Leukemia (JMML) is closely associated with fetal development. Nevertheless, the contribution of embryonic progenitors to JMML pathogenesis remains unexplored. We hypothesized that expression of JMML-initiating PTPN11 mutations in HSC-independent yolk sac erythromyeloid progenitors (YS EMPs) would result in a mouse model of pediatric myeloproliferative neoplasm (MPN).

**Results—**E9.5 YS EMPs from VavCre+;PTPN11$^{D61Y}$ embryos demonstrated growth hypersensitivity to GM-CSF and hyperactive RAS-ERK signaling. Mutant EMPs engrafted the spleens of neonatal recipients, but did not cause disease. To assess MPN development during unperturbed hematopoiesis we generated CSF1R-MCM+;PTPN11$^{E76K}$;ROSA$^{YFP}$ mice in which oncogene expression was restricted to EMPs. YFP+ progeny of mutant EMPs persisted in tissues one year after birth and demonstrated hyperactive RAS-ERK signaling. Nevertheless, these mice had normal survival and did not demonstrate features of MPN.

**Conclusions—**YS EMPs expressing mutant PTPN11 demonstrate functional and molecular features of JMML but do not cause disease following transplantation nor following unperturbed development.

Correspondence: Mervin C. Yoder, 1044 W. Walnut Street, R4-125, Indianapolis, Indiana 46202, USA. Phone: 317-274-4738; myoder@iu.edu.

Present address: Center for Stem Cell and Regenerative Medicine, Brown Foundation Institute of Molecular Medicine, University of Texas Health Science Center at Houston, Houston, TX 77030, USA

**Conflict of interest statement**: The authors have declared that no conflict of interest exists.

**Authorship Contributions**: SPT conceived the study, designed, performed, and analyzed experiments, and wrote the manuscript. MY designed, performed, and analyzed experiments. LD performed experiments. RJC and MCY conceived the study, designed and analyzed experiments, and edited the manuscript. All authors read and approved the manuscript.

## Introduction

Juvenile Myelomonocytic Leukemia (JMML) is a pediatric myeloproliferative neoplasm (MPN) caused by mutations in RAS-ERK signaling genes. Gain of function PTPN11 mutations are the most frequent cause of JMML, and are present in ~35% of cases (Sakaguchi et al., 2013; Caye et al., 2015; Stieglitz et al., 2015). Patients suffer from monocytosis, anemia, thrombocytopenia, hepatosplenomegaly, and have a poor overall survival (Chan et al., 2009b; Locatelli and Niemeyer, 2015). Recent evidence has implicated a developmental origin to this disease. Children present very young with a median age of <2 years. Patients frequently have elevated levels of fetal hemoglobin and their bone marrow cells have a gene expression signature characteristic of fetal progenitors (Weinberg et al., 1990; Helsmoortel et al., 2016). Furthermore, retrospective analysis suggests that the majority of somatic JMML-initiating mutations occur before birth (Kratz et al., 2005; Matsuda et al., 2010; Stieglitz et al., 2015). Nevertheless, the identity of the JMML-initiating cell remains controversial.

The first murine hematopoietic stem cell (HSC) emerges around E11.0 in the aorta-gonad-mesonephros region (Muller et al., 1994; Boisset et al., 2010). The HSC migrates to the fetal liver, expands, and seeds the bone marrow around birth (Christensen et al., 2004). The emergence of HSCs is preceded by sequential waves of hematopoiesis that originate in the extraembryonic yolk sac (YS) and consist primarily but not exclusively of progenitors with limited differentiation and self-renewal potential (Frame et al., 2013; Lin et al., 2014). The first HSC-independent wave consists of bipotent megakaryocytic-erythroid progenitors (MEP) and myeloid-restricted progenitors (Mac-CFC) (Moore and Metcalf, 1969; Bertrand et al., 2005; Tober et al., 2007). These arise directly from mesoderm around E7.0 and are termed primitive due to their morphology. A second HSC-independent wave begins around E8.25 with the emergence of erythromyeloid-progenitors (EMPs) via an endothelial-to-hematopoietic transition (Palis et al., 1999; Lux et al., 2008; Frame et al., 2016). EMPs seed the fetal liver around E10.5 where they give rise to enucleated erythrocytes and diverse myeloid progeny including neutrophils, monocytes, and macrophages (Chen et al., 2011; McGrath et al., 2015). Following EMPs, lymphoid restricted progenitors and multilineage neonatal repopulating cells emerge in the YS prior to the first HSC (Yoder et al., 1997; Yoshimoto et al., 2010; Yoshimoto et al., 2012).

Recent evidence has highlighted the importance of EMPs in development. EMPs are integral for *in utero* vascular remodeling and sterile inflammatory signals from EMP-derived myeloid progeny promote the emergence of HSCs (DeFalco et al., 2014; Espin-Palazon et al., 2014; Li et al., 2014; Kasaai et al., 2017). Furthermore, loss of EMPs is not compatible with life since their progeny are required to sustain the embryo during the late fetal period when HSC-dependent progenitors are proliferating (Mucenski et al., 1991). Finally, whereas initial studies suggested EMPs had a transient role in development, recent work has proven that the progeny of EMPs persist into adulthood as tissue resident macrophages (Samokhvalov et al., 2007; Ginhoux et al., 2010; Schulz et al., 2012; Kierdorf et al., 2013; Epelman et al., 2014; Gomez Perdiguero et al., 2015; Hoeffel et al., 2015). YS-derived macrophages are present in the majority of organs at birth, and undergo gradual replacement by HSC-derived progeny. The rate of this replacement varies by tissue; it is very rapid in the

gut, whereas it is delayed in the spleen, liver, and heart. Importantly, there is negligible replacement of brain YS-derived macrophages. The majority of microglia retain an embryonic origin life-long, even after HSC transplant (HSCT) (Kennedy and Abkowitz, 1997; Ginhoux et al., 2010; Hashimoto et al., 2013).

The contribution of YS progenitors to JMML is unknown. Several lines of evidence—in addition to the disease's *in utero* origin and fetal characteristics—suggest that EMPs may contribute to the pathogenesis of this disease. JMML has been successfully modelled with patient-derived induced pluripotent stem cells (iPSCs) (Gandre-Babbe et al., 2013; Mulero-Navarro et al., 2015). However, iPSCs cannot give rise to HSCs and can only recapitulate YS-like HSC-independent hematopoiesis (Vanhee et al., 2015; Buchrieser et al., 2017). This suggests that YS-derived progeny will have defining features of JMML. Additionally, whereas HSCT is the only curative treatment for JMML, up to 52% of patients will relapse (Locatelli et al., 2005; Olk-Batz et al., 2011) suggesting that malignant JMML cells are uniquely resistant to myeloablation. Since tissue resident macrophages in both mice and humans are also relatively resistant to myeloablation, we hypothesized that EMPs may contribute to JMML relapse via their long-lived myeloid progeny (Kennedy and Abkowitz, 1997; Haniffa et al., 2009; Hashimoto et al., 2013).

Previous studies have struggled to identify the contribution of YS progenitors to disease. One study used transplantation experiments to evaluate the HSC-dependent vs. HSC-independent origin of tumor-associated macrophages (Gordon et al., 2017). However, transplantation is not a reliable approach since YS-derived macrophages outside the brain are gradually replaced by donor contributions – albeit at a slower rate than HSC-derived myeloid populations. Other studies have assessed the aberrant function of mutation-expressing YS progenitors *ex vivo* and have shown them to have unique disease phenotypes. For instance, YS-derived megakaryocytes are uniquely hyperproliferative following expression of truncated GATA1 (Li et al., 2005). However, this study was not able to assess the postnatal consequences of mutations restricted to YS progenitors.

In our study, we use complementary approaches to evaluate the consequences of JMML-associated gain-of-function PTPN11 mutations in EMPs. In addition to *ex vivo* assays and transplantation experiments, we take advantage of inducible lineage tracing Cre-loxP techniques to study the postnatal effects of mutant EMPs. We thereby definitively address our hypothesis that restricted expression of mutant PTPN11 in YS EMPs will be sufficient for the emergence of MPN in a mouse model of JMML. We demonstrate that YS EMPs expressing gain-of-function PTPN11 have defining features of JMML, including growth hypersensitivity to GM-CSF and RAS-ERK hyperactivation. Nevertheless, mutant YS EMPs were not able to give rise to MPN following transplantation nor following unperturbed development despite the durable persistence of their progeny in adult mice.

## Results

We hypothesized that *in utero* expression of the PTPN11$^{D61Y}$ JMML-initiating mutation would result in the rapid onset of MPN in mice. To test this hypothesis we activated the oncogene in early hematopoietic progenitors using VavCre, whose expression begins in fetal

blood cells (Ghiaur et al., 2008). VavCre+; PTPN11$^{D61Y}$ mice were viable and born at expected Mendelian ratio (Fig-1A), developed leukocytosis and monocytosis by 8 weeks of age, and had a median survival of 31 weeks (Fig-1B). Given that Mx1Cre+;PTPN11$^{D61Y}$ mice have a reported median survival of 45 weeks, our results suggest that oncogene expression by *in utero* progenitors exacerbates progression of PTPN11$^{D61Y}$-induced MPN (Chan et al., 2009a).

To confirm that embryonic progenitors expressing PTPN11$^{D61Y}$ manifested features of MPN, we assayed their growth in methylcellulose medium with increasing doses of GM-CSF. Both E14.5 fetal liver (FL) progenitors and E9.5 YS progenitors from VavCre +;PTPN11$^{D61Y}$ mutant embryos had markedly greater colony formation at low doses of GM-CSF compared to littermate controls (Fig-1C,D). To evaluate if this GM-CSF hypersensitivity was due to hyperactive RAS signaling, we measured the phosphorylation (p-) of ERK. Mutant cells cultured from E14.5 FL had markedly elevated p-ERK levels both at baseline and following 30min stimulation with 10ng/ml GM-CSF, as measured by western blot (Fig-1E). Additionally, mutant cells cultured from E9.5 YS also had elevated p-ERK and p-STAT5 levels as measured by intracellular flow cytometry (Fig-1F). These results demonstrate that both HSC-dependent FL progenitors and HSC-independent YS cells have defining functional features of JMML. To determine the identity of the hyperactive YS progenitor, we sorted Ter119- CD41$^{dim}$ cKit+ YS EMPs from E9.5 VavCre+;PTPN11$^{D61Y}$ mutants and littermate controls. Mutant EMPs produced greater numbers of colonies at the tested concentrations of GM-CSF (Fig-1G), providing evidence that the EMP is the YS progenitor responsible for the observed features of JMML.

Tissue macrophages are the durable progeny of EMPs and they are relatively resistant to myeloablation compared to other myeloid cells. As such, mutant EMPs may contribute to JMML relapse following HSCT via their myeloablation-resistant progeny. To test this notion, we devised a therapeutic HSCT in which VavCre+;PTPN11$^{D61Y}$ mice were treated with adoptive transfer of healthy CD45.1+ BM cells (Fig-2A). We hypothesized that recipients would relapse following poor donor engraftment. We transplanted 12-24week old lethally irradiated mutant and littermate animals (CD45.2+) with $5\times10^5$ heathy congenic CD45.1+ BM cells. We were surprised to observe that donor cells engrafted more readily in mutant recipients than in control recipients (Fig-2B). Furthermore, the engrafted cells preferentially gave rise to CD11b+ myeloid cells and to fewer CD3+ T-lymphocytes (Fig-2C). Despite this robust engraftment, mutant recipient mice rapidly succumbed after transplantation, with a mean survival of 16 weeks (Fig-2D). To evaluate whether limiting donor cell numbers affected post-transplant survival, we repeated the experiment using $1\times10^7$ CD45.1+ donor BM cells. Mutant mice nevertheless succumbed with a median survival of 18 weeks (Fig-2D).

At analysis, moribund mutant recipients had a hypercellular BM with an effacement of the normal splenic follicular architecture (Fig-2F,G). We were surprised, however, to find markedly enlarged thymuses in moribund mutants (not shown). Subsequent analysis confirmed that both the BM and spleen were filled with CD45.2+ recipient-derived CD4+ CD8+ cells, which are indicative of T-cell leukemia/lymphoma (T-ALL) (Fig-2E). Transplantations of BM and spleen cells from HSCT-treated mutants into CD45.1 recipients

confirmed that the CD45.2+ T-ALL disease could be propagated and was neoplastic (not shown). From these experiments we concluded that healthy donor cells could efficiently engraft mutant recipients and preferentially gave rise to myeloid progeny. Despite this robust engraftment, mutants died after transplantation due to the emergence of a recipient-derived T-ALL, which could be propagated upon transplantation. Importantly, this finding contrasts with JMML patients who rarely demonstrate emergence of T-ALL and primarily relapse with MPN following HSCT (Cooper et al., 2000).

PTPN11$^{D61Y}$ murine models have indolent disease progression. We reasoned that a different JMML-associated PTPN11 mutation that causes more rapid disease onset would help accentuate our findings. We chose the conditional PTPN11$^{E76K}$ mouse because it succumbs to MPN more rapidly than PTPN11$^{D61Y}$ mice and because this mutation has been documented to occur *in utero* in JMML patients (Matsuda et al., 2010; Xu et al., 2011).

Sorted YS EMPs from E10.0 VavCre+;PTPN11$^{E76K}$ were growth hypersensitive to GM-CSF, further demonstrating that mutated HSC-independent progenitors have features of JMML (Fig-3A). Surprisingly, when we mated VavCre mice with PTPN11$^{E76K/+}$ mice we did not obtain viable VavCre+;PTPN11$^{E76K}$ progeny (Fig-3C). Analyses of E10.5 embryos showed mutants were smaller, less developed, and had a pale YS and AGM region (Fig-3D). Subsequent analysis of E17.5 embryos confirmed that VavCre+;PTPN11$^{E76K}$ embryos were dying *in utero* (Fig-3D). This was in contrast to recent publications that reported this model to be viable and develop MPN (Dong et al., 2016; Liu et al., 2016). This discrepancy is likely due to the use of different VavCre strains. Prior studies used the VavCre$^{Stadtfeld}$ strain, which has minimal expression in endothelial and stromal cells. In contrast, the VavCre$^{Croker}$ and VavCre$^{deBoer}$ strains in our studies have pronounced expression in endothelial cells which may cause the prenatal lethality we observed (de Boer et al., 2003; Croker et al., 2004; Stadtfeld et al., 2007).

Despite the *in utero* lethality of VavCre$^{Croker}$;PTPN11$^{E76K}$ mice, their E10.0 YS hematopoietic progenitors gave rise to a normal distribution of BFU-E, CFU-GM, and CFU-GEMM colonies (Fig-3B). We therefore tested whether YS progenitors could give rise to MPN upon transplantation. We transplanted 1 embryo equivalent (e.e.) FACS-sorted YS EMPs from E10.5 VavCre+;PTPN11$^{E76K}$ embryos i.v. into 150cGy sublethally irradiated neonatal NSG CD45.1+ recipients. We also transplanted CD45- Ter119- cKit+ VE-Cadherin + hemogenic endothelial populations from the AGM of the same embryos (Rybtsov et al., 2011). Prior work has demonstrated neonatal recipients are uniquely capable of supporting YS progenitor engraftment (Yoder and Hiatt, 1997; Yoder et al., 1997; Yoshimoto et al., 2010; Yoshimoto et al., 2012; Arora et al., 2014). Nonetheless, we did not observe peripheral blood engraftment or elevated leukocyte counts in recipients of either YS or AGM cells (Fig-3E). This finding is consistent with recent studies that showed purified YS EMPs did not contribute to circulating leukocytes following transplantation (McGrath et al., 2015).

At tissue analysis 18 weeks post-transplant, we were surprised to discover that donor EMPs had engrafted in recipient spleens as F4/80$^{+}$ CD11b$^{dim}$ macrophages (Fig-3F). The engraftment of splenic macrophages was more robust in recipients of YS EMPs than of AGM VECad+ cells. Notably, whereas the most prominent progeny of EMPs are microglia,

we did not detect any CD45.2+ cells in the brains of EMP recipients (Fig-3G). These results are consistent with previous studies that showed differences in progenitor differentiation under native and transplant settings (Boyer et al., 2011; Busch et al., 2015). Our findings highlight the pitfalls of models that rely on transplantation, which identify progenitor potentials under non-native conditions (Schlenner and Rodewald, 2010; Busch and Rodewald, 2016). We concluded that it would not be feasible to definitively evaluate the contribution of HSC-independent progenitors to JMML using the VavCre model.

We therefore turned to the CSF1R Mer-Cre-MER (MCM) model which can restrict Cre activity to YS EMPs following 4-hydroxytamoxifen (4OHT) injection of pregnant dams at E8.5 (Qian et al., 2011; Gomez Perdiguero et al., 2015). We mated CSF1R-MCM +;$ROSA^{YFP/YFP}$ studs with $PTPN11^{E76K/+}$ dams to generate mutant CSF1R-MCM;$ROSA^{YFP/+}$;$PTPN11^{E76K/+}$ progeny (CSF1R-MCM;$PTPN11^{E76K}$) (Fig-4A). In these animals, Cre-mediated recombination results in the expression of both $PTPN11^{E76K}$ and yellow fluorescent protein (YFP). As such, cells expressing the oncogene can be monitored using flow cytometry. 24 hours after oncogene activation by 4OHT injection, mutant and littermate embryos had equal frequencies of YS EMPs (Fig-4B). Additionally, the frequency of YFP+ EMPs was equivalent in both mutants and controls. (Fig-4C). This indicated that mutants and littermates had equivalent activity of the Cre recombinase. We proceeded to assess proliferation of EMPs using Ki67 staining. EMPs from mutant YS did not have increased Ki67 expression compared to their littermates (Fig-4D). Additionally, p-ERK levels in both YFP+ and YFP- EMPs from mutant embryos was not increased following GM-CSF stimulation compared to control EMPs (Fig-4E). The lack of cell cycle and signaling differences may be attributed to the highly proliferative nature of embryonic hematopoietic progenitors as compared with their adult counterparts (Bowie et al., 2007). We reasoned that any oncogenic effects of $PTPN11^{E76K}$ mutation would only be evident postnatally, once hematopoietic progenitors enter a state of relative quiescence.

We proceeded to generate a cohort of CSF1R-MCM; $PTPN11^{E76K}$ animals that had been exposed to 4OHT at E8.5 (Figure-5A). Mutants were weaned at a normal Mendelian frequency of 24% and were physically indistinguishable from littermates (Fig-5B). We monitored all animals in this cohort with monthly peripheral blood draws (Fig-5C-G). As expected, we did not observe YFP+ cells in the peripheral blood, indicating that Cre was not active in HSCs. Over a 52 week period, we did not observe leukocytosis, anemia, or thrombocytopenia in mutant animals. Furthermore, we did not see evidence of myeloproliferation or skewing of leukocyte lineages. Over the course of the study, one mutant animal succumbed from an unclear cause and one littermate control succumbed to sporadic T-ALL (Fig-5H).

We considered that indolent MPN progression in these animals may not manifest in the peripheral blood and would only be evident upon tissue examination. We hypothesized that mutant adults would have a greater frequency of YFP+ macrophages compared to controls due to growth promoting effects of $PTPN11^{E76K}$. However, upon analysis, mutant animals did not have hepatosplenomegaly and no YFP+ cells were detected in the BM and spleen (Fig-6A,B). Additionally, mutant animals had a normal distribution of leukocyte lineages in the BM and spleen, indicating absence of myeloid-biased differentiation. (Fig-6C,D).

We proceeded to characterize macrophage populations in the brain, heart, and liver; the tissues with the greatest contribution from YS EMPs. Consistent with previous reports we saw high proportions of YFP+ microglia and measureable proportions of YFP+ heart and liver macrophages (F4/80$^{bright}$ CD11b+) (Fig-6E,F). Nonetheless, we did not observe differences in the frequency of YFP+ macrophages between CSF1R-MCM; PTPN11$^{E76K}$ and controls in any tissue. To determine whether the former presence of mutant splenic macrophages had evoked GM-CSF hypersensitivity in progenitors we performed colony forming assays. No difference in colony formation was observed between mutant and littermate samples (Fig-6G). To ensure that the PTPN11$^{E76K}$ allele was appropriately recombined, we confirmed the excision of the loxP-STOP-loxP cassette in brains of mutant animals (Fig-6H). We then assayed RAS-ERK signaling in freshly-isolated mutant and control microglia and confirmed that mutant cells had greater p-ERK levels (Fig-6J). These results suggest that *in utero* PTPN11$^{E76K}$ expression by YS EMPs gives rise to tissue macrophage populations with hyperactive RAS-ERK signaling that persist more than a year after birth. Nevertheless, these mutant EMPs did not cause overt signs of MPN such as monocytosis, anemia, and hepatosplenomegaly.

## Discussion

We present the first study to directly assess the contribution of HSC-independent hematopoietic progenitors to pediatric neoplasms. We show that YS EMPs expressing mutant PTPN11 are hypersensitive to GM-CSF and have hyperactive RAS-ERK signaling. Nevertheless, EMPs expressing gain-of-function PTPN11 do not cause disease upon transplantation nor following *in utero* expression using the tamoxifen-inducible CSF1R-MCM system.

Recent studies have provided tantalizing evidence for the potential contribution of embryonic HSC-independent hematopoiesis to JMML. The strikingly high relapse rate following HSCT suggests that myeloablation-resistant and HSC-independent populations contribute to disease emergence (Locatelli et al., 2013). YS EMPs admirably match these criteria: they give rise to tissue macrophage populations in diverse tissues that are long-lived and relatively resistant to myeloablation (Haniffa et al., 2009; Hashimoto et al., 2013; Epelman et al., 2014; Gomez Perdiguero et al., 2015). Second, JMML patients frequently acquire their disease-initiating mutations *in utero* (Matsuda et al., 2010; Stieglitz et al., 2015). Finally, several studies have successfully modelled JMML using patient-derived iPSCs, whose differentiation mimics that of HSC-independent YS hematopoiesis (Gandre-Babbe et al., 2013; Mulero-Navarro et al., 2015; Vanhee et al., 2015; Buchrieser et al., 2017). This reasoning prompted us to hypothesize that expression of JMML-initiating mutations in embryonic HSC-independent progenitors would be sufficient for disease development (Chan and Yoder, 2013).

Our initial experiments with VavCre+;PTPN11$^{D61Y}$ mice demonstrated the feasibility of this hypothesis. These animals rapidly succumbed to MPN and their HSC-independent YS EMPs had two disease-defining features of JMML: growth hypersensitivity to GM-CSF and hyperactive RAS-ERK signaling. This suggested that YS progenitors may contribute to MPN emergence. However, transplantation of VavCre+;PTPN11$^{E76K}$ EMPs did not cause

disease in neonatal NSG recipients despite robust engraftment as splenic macrophages. The inability of mutant macrophages to cause disease further demonstrates that the aberrant peripheral monocytes in MPN are distinct from tissue macrophages. This finding is consistent with a growing literature that highlights functional, morphologic, and transcriptional differences between circulating and resident myeloid cells (Lavin et al., 2014). Importantly, ours is the first study to demonstrate durable engraftment of EMPs following transplantation. Previous studies showed that transplantation of EMPs into adult recipients resulted in transient erythroid contributions but not leukocyte engraftment (McGrath et al., 2015). It is unclear, however, whether our engraftment was the result of oncogene-expressing EMPs or whether it was enabled by the use of neonatal recipients. Future studies will need to evaluate whether mutant PTPN11 or recipient age is the major determining factor permitting EMP engraftment.

Our study further highlights the challenges of transplantation experiments in studying disease initiating cells. The dominant progeny of EMPs in unperturbed hematopoiesis are microglia. Nevertheless, we observed EMP engraftment in the spleen but not the CNS following neonatal transplantation. Differences between *in vivo* differentiation and transplantation-evoked potentials among adult hematopoietic progenitors have also been shown (Schlenner and Rodewald, 2010; Busch and Rodewald, 2016). Additionally, we saw that VavCre+;PTPN11$^{D61Y}$ mice engrafted with healthy donor cells had disease exacerbation and rapidly succumbed to recipient-derived T-ALL. In contrast, non-irradiated animals expressing PTPN11$^{D61Y}$ die from MPN (Chan et al., 2009a). Our findings are consistent with other studies that showed frequent T-ALL emergence in irradiated mutant PTPN11-expressing animals due to impaired DNA repair (Liu et al., 2016). As such, our results emphasize that the same mutation may give rise to divergent disease manifestations in irradiated and non-irradiated animals.

Previous studies have implicated an abnormal hematopoietic microenvironment in the pathogenesis of JMML (Xu et al., 2013; Dong et al., 2016). This group demonstrated that non-mutated progenitors that occupy a mutant PTPN11-expressing niche have features of MPN including hyperactive RAS-ERK signaling and myeloid-biased differentiation. Our finding that healthy donor progenitors preferentially contribute to CD11b+ myeloid cells following transplantation into VavCre+;PTPN11$^{D61Y}$ animals is consistent with these earlier findings. Additionally, we show that disease reemergence in mutant animals following healthy donor HSCT is not caused by impaired engraftment. Rather, the greater frequency of CD45.1+ leukocytes in VavCre+;PTPN11$^{D61Y}$ recipients compared to controls suggests that that the mutant niche may evoke increased cycling among donor progenitors, potentially leading to premature exhaustion.

Our *ex vivo* analyses and transplantation experiments demonstrate the challenges of measuring the contribution of HSC-independent progenitors to disease. Previous studies also relied on transplantation experiments and/or isolation of *in utero* progenitors (Li et al., 2005; Gordon et al., 2017). However, these approaches prevent the analysis of postnatal effects of prenatal mutations. Our major advance was to adapt the lineage-tracing CSF1R-MCM system to restrict the expression of PTPN11$^{E76K}$ to EMPs and permit the normal birth and development of these mice. The concomitant use of the ROSA$^{YFP}$ reporter enabled us to

analyze the frequency and functional characteristics of mutant EMP progeny. We were thus able to show that mutant EMPs in CSF1R-MCM+;PTPN11$^{E76K}$ embryos did not have enhanced proliferation or hyperactive RAS-ERK signaling compared to littermates. After birth, no YFP+ EMP progeny were observed in the peripheral blood and no evidence of MPN was detected during year-long monitoring despite the persistence of YFP+ mutant macrophages in the brain, liver, and heart. Microglia in mutants had recombined their PTPN11$^{E76K}$ locus and had hyperactive RAS-ERK signaling. Nevertheless, these animals did not have diminished survival and they did not show signs of morbidity.

There are several possible explanations for the lack of disease in our cohorts. First, YS EMPs may not possess the differentiation potential required for fulminant MPN emergence. Indeed, whereas EMPs do give rise to neutrophils and monocytes, their long lived progeny are tissue resident macrophages, which are functionally, transcriptionally, and epigenetically distinct from the circulating myeloid populations that are expanded in JMML patients (Gosselin et al., 2014; Lavin et al., 2014). Additionally, healthy EMPs may already be so proliferative that PTPN11$^{E76K}$ had no effect on their cell cycle, as measured by Ki67. Furthermore, only 35% of E9.5 EMPs were targeted in our model. This is a much lower frequency than the >90% efficiency obtained from most conditional mouse models, such as Mx1Cre or VavCre. Finally, the CSF1R-MCM can only label EMPs between E8.5 and E9.5 (Gomez Perdiguero et al., 2015; Hoeffel et al., 2015). In contrast, the transcriptional program that drives the emergence of EMPs begins between E6.5-E7.5, the first EMPs emerge at E8.25, continue to arise until at least E10.5, and proliferate until birth (Chen et al., 2011; Tanaka et al., 2012; Tober et al., 2013). As such, our system labels only a minority of one subset of EMPs and it is possible that other HSC-independent progenitors, including distinct EMP subpopulations and neonatal repopulating cells, may respond differently when expressing PTPN11 mutations (Yoder et al., 1997; Sheng et al., 2015; Frame et al., 2016).

In conclusion, we present the first study to evaluate the contribution of HSC-independent hematopoietic progenitors to JMML. We show that YS EMPs expressing gain-of-function PTPN11 are hypersensitive to GM-CSF and have hyperactive RAS-ERK signaling. Nevertheless, mutant EMPs were not able to give rise to disease upon transplantation nor in the context of unperturbed development. Our findings suggest YS EMPs may be resistant to transformation by this mutation. We conclude that PTPN11$^{E76K}$ expression in a subset of YS EMPs does not result in an expansion of mutant macrophages and is not sufficient for MPN emergence in a mouse model of JMML.

## Experimental Procedures

### Mice

C57BL/6J, B6.SJL-Ptprca Pepcb/ (BoyJ), and NOD.Cg-Prkdcscid Il2rgtm1Wjl/SzJ (NSG) mice were bred in-house. LSL-PTPN11$^{D61Y/+}$ mice were obtained from Dr. Gordon Chan and Dr. Benjamin Neel (U. Toronto, Canada). LSL-PTPN11$^{E76K/+}$ mice were obtained from Dr. Cheng-Kui Qu (U. Emory, Atlanta, GA). ROSA$^{YFP/YFP}$ mice were obtained from Dr. Anthony Firulli (IUSM, Indianapolis, IN). CSF1R-Mer-Cre-Mer mice (#019098) were purchased from Jackson Labs and were back-crossed onto the C57B6 background for 6 generations. VavCre$^{Croker}$ mice were mated with PTPN11$^{E76K}$ and were a gift from Dr.

David Williams (Boston Children's Hospital, Boston, MA). VavCre$^{deBoer}$ mice were mated with PTPN11$^{D61Y}$ and were a gift from Dr. Reuben Kapur (IUSM, Indianapolis, IN). Mice were identified by ear notches or toe clips. Genotyping was performed with conventional PCR using primers listed in the Appendix. Experimental and control animals were housed together in the same cages. All animal studies were performed with prior approval from the IUSM Institutional Animal Care and Use Committee.

### Mouse hematologic analysis

Blood collections were done via tail vein into EDTA-coated tubes (Fisher #NC9628695). Counts were obtained using a HemaVet 950 (Drew Scientific). Blood smears and cytospins were stained using Modified Wright-Giemsa dyes on a Hematek 3000 system (Siemens). For subsequent flow cytometric analysis, up to 60ul of blood was aliquoted into 1ml of Blood Collection Medium (IMDM +10%FBS +1% Pen/Strep + 20U/ml Heparin (Sigma #H3149)).

### Timed Matings

Male studs (10-26 weeks of age) were housed in separate cages and mated after at least 2-3 days of acclimatization to their cage. In the evening one or two female mice (8-26 weeks of age) were moved to the stud cage. The following morning, successful matings were confirmed by visual inspection of a vaginal plug and assigned a gestational age of E0.5.

### Tamoxifen Treatment

To induce recombinase activity in utero, pregnant dams were injected i.p. with 75ug/g 4-hydroxy tamoxifen (Sigma #H6278) along with 37.5ug/g progesterone (Sigma #P0130). Litters of tamoxifen-treated dams were routinely delivered by C-section on E19.5 and raised by foster females.

### Embryo Harvests

Pregnant females were euthanized by cervical dislocation followed by bilateral pneumothorax. The abdominal cavity was opened using sterile scissors and forceps. The uterine horns were removed and placed in a petri dish with sterile PBS. The uterine fascia, musculature, and placental tissues were sequentially removed using forceps to expose the YS-enclosed embryo. Embryo age was confirmed by counting somite pairs: E9.5 (20-26sp), E10.0 (27-32sp), E10.5 (33-37sp). Desired tissues were dissected out and placed into collection tubes containing PBS. Tissue digests were performed for 5-30min at 37°C in 0.125% collagenase type I (Stem Cell Technologies #07902).

### Ex Vivo Culture

Cells were cultured in a humidified incubator at 37°C, 5% $CO^2$ in IMDM (Fisher #12440079), 10% FBS (Fisher #SH30070.03), 100 U/ml Penicillin/Streptomycin (Fisher #15140122), 440nM β-Mercaptoethanol (Sigma #M6250), and 2mM L-Glutamine (Fisher # 25030-081). Yolk sac or fetal liver cells were differentiated into macrophages by culturing for 7 days in 10ng/ml M-CSF (Peprotech #315-02).

### Hematopoietic Cell Isolations

All tissues were kept on ice in PBS +2mM EDTA. Bone marrow cells were flushed from hindlimb bones. Spleens were triturated with glass cover slides. Livers, hearts, and brains were minced with razors and digested at 37°C in 0.2% collagenase D (Sigma #11088866001), 0.5% Dispase (Fisher #17105-041) and 50U/ml DNase I (Sigma #10104159001) for 60min. Enucleated RBCs were depleted as necessary using density gradient centrifugation in Histopaque (Sigma #10771) or RBC lysis buffer (Quiagen #158904). As needed, liver and brain suspensions were depleted of parenchymal cells and lipids via centrifugation through a 37% and 50% Percoll (Sigma #P1644) gradient, respectively.

### Flow Cytometry

Cells were stained at a concentration of 1-5 × $10^7$/ml in PBS +2% FBS + 2mM EDTA. Antibody concentrations were determined experimentally. If required, cells were fixed in 1% PFA (Fisher #50-980-487). For cell cycle analysis, stained cells were permeabilized with eBioscience Intracellular Fixation & Permeabilization Buffer Set (#88-8824-00). For Intracellular phospho-flow, cells were stimulated in an Eppendorf tube with GM-CSF (Peprotech #315-03), fixed in 1% PFA for 15min, and permeabilized using BD Perm Buffer III (#558050). Stained cells were analyzed using the BD LSR Fortessa, BD FACS CANTO II, or BD Accuri C6. Post run analysis was performed using FlowJo (Treestar).

### Tissue Histopathology

Tissue samples were fixed in 4% PFA, dehydrated with ethanol, cleared with xylenes and embedded in paraffin. 5um sections were cut on a rotary microtome and stained with hematoxylin and eosin.

### DNA isolation

Murine tails were digested for 1hr at 95°C in 50mM NaOH + 0.2mM EDTA, vortexed, pelleted, and then diluted to 100mM Tris buffer. Alternatively, DNA was isolated from tissues using the DNeasy Blood & Tissue Kit (Quiagen # 69504).

### Hematopoietic Progenitor Colony Forming Assay

$2×10^4$ FL mononuclear cells, $2.5 ×10^5$ spleen cells or 1/5 of total YS cells were plated in 1ml of 30% methylcellulose in IMDM (Stemcell Technologies #M3120) supplemented with 30% FBS, 2.2% Pen/Strep, 2.45mM L-Glutamine, and 440nM β-Mercaptoethanol (Sigma #M6250) and defined concentration of murine GM-CSF.

### Transplantations

Adult recipients (8-24wks) were lethally irradiated with 700cGy+400cGy. Within 16hrs, donor cells were adoptively transferred via tail vein in 250ul PBS using a 28G insulin syringe (Fisher #BD 329461). A heat lamp and alcohol swab was used to engorge the vein. Neonatal NSG recipients (2 day-old) were sublethally irradiated with 150cGy. Immediately after irradiation, donor cells were adoptively transferred via facial vein in 30ul PBS using a 30G needle and a 0.1ml syringe (Hamilton #1710).

### Western blots

Protein extracts were obtained by lysing cultured or primary cells for 30min on ice in 50mM HEPES, 150mM NaCl, 10% Glycerol, 1% Triton X100, 1.5mM MgCl2, 1mM EGTA, 100mM NaF, 10mM NaPP, along with a protease inhibitor cocktail containing sodium vanadate, ZnCl2, PMSF (Sigma # 93482), and enzymatic inhibitors (Sigma # 10837091001). Protein lysates were run using SDS-PAGE, transferred to nitrocellulose membranes. Blots were exposed using SuperSignal West Pico Chemiluminescent Substrate (Fisher #34080).

### Statistical analyses

P-values were calculated using Graph Pad Prism 7.0. Two-tailed t-tests were used to compare two-variable experiments. Chi-squared analyses were used to compare birth ratios. Survival analyses were performed by Mantel-Cox log-rank tests. Two-way ANOVA analyses were used to compare changes in variables over time. All error bars represent SEM. P values <0.05 were considered significant. Notation: * p-value<0.05; ** p-value<0.01; *** p-value<0.001; ns not significant.

## Supplementary Material

Refer to Web version on PubMed Central for supplementary material.

## Acknowledgments

We are grateful to Dr. Michelle Block for helpful discussions. This work was supported by the U.S. National Institutes of Health (F30 HL128011 to SPT and R21 CA202296 to RJC, MCY), the IU Simon Cancer Centre (2289903 to RJC, MCY), and the Riley Children's Foundation. We appreciate the technical assistance from Dr. Karen Pollok and Tony Sinn in the Indiana University In Vivo Therapeutics Core and Susan Rice in the Flow Cytometry Resource Facility (supported by P30 CA082709). The authors gratefully acknowledge the administrative assistance of Tracy Winkle and Tiffany Lewallen.

This work was supported by the U.S. National Institutes of Health (F30 HL128011 to SPT and R21 CA202296 to RJC, MCY), the IU Simon Cancer Centre (2289903 to RJC, MCY), and the Riley Children's Foundation. We appreciate the technical assistance from Dr. Karen Pollok and Tony Sinn in the Indiana University In Vivo Therapeutics Core and Susan Rice in the Flow Cytometry Resource Facility (supported by P30 CA082709).

## References

Arora N, Wenzel PL, McKinney-Freeman SL, Ross SJ, Kim PG, Chou SS, Yoshimoto M, Yoder MC, Daley GQ. Effect of Developmental Stage of HSC and Recipient on Transplant Outcomes. Dev Cell. 2014; 29:621–628. [PubMed: 24914562]

Bertrand JY, Jalil A, Klaine M, Jung S, Cumano A, Godin I. Three pathways to mature macrophages in the early mouse yolk sac. Blood. 2005; 106:3004–3011. [PubMed: 16020514]

Boisset JC, van Cappellen W, Andrieu-Soler C, Galjart N, Dzierzak E, Robin C. In vivo imaging of haematopoietic cells emerging from the mouse aortic endothelium. Nature. 2010; 464:116–120. [PubMed: 20154729]

Bowie MB, Kent DG, Dykstra B, McKnight KD, McCaffrey L, Hoodless PA, Eaves CJ. Identification of a new intrinsically timed developmental checkpoint that reprograms key hematopoietic stem cell properties. Proc Natl Acad Sci U S A. 2007; 104:5878–5882. [PubMed: 17379664]

Boyer SW, Schroeder AV, Smith-Berdan S, Forsberg EC. All hematopoietic cells develop from hematopoietic stem cells through Flk2/Flt3-positive progenitor cells. Cell Stem Cell. 2011; 9:64–73. [PubMed: 21726834]

Buchrieser J, James W, Moore MD. Human Induced Pluripotent Stem Cell-Derived Macrophages Share Ontogeny with MYB-Independent Tissue-Resident Macrophages. Stem Cell Reports. 2017; 8:334–345. [PubMed: 28111278]

Busch K, Klapproth K, Barile M, Flossdorf M, Holland-Letz T, Schlenner SM, Reth M, Hofer T, Rodewald HR. Fundamental properties of unperturbed haematopoiesis from stem cells in vivo. Nature. 2015; 518:542–546. [PubMed: 25686605]

Busch K, Rodewald HR. Unperturbed vs. post-transplantation hematopoiesis: both in vivo but different. Curr Opin Hematol. 2016; 23:295–303. [PubMed: 27213498]

Caye A, Strullu M, Guidez F, Cassinat B, Gazal S, Fenneteau O, Lainey E, Nouri K, Nakhaei-Rad S, Dvorsky R, Lachenaud J, Pereira S, Vivent J, Verger E, Vidaud D, Galambrun C, Picard C, Petit A, Contet A, Poiree M, Sirvent N, Mechinaud F, Adjaoud D, Paillard C, Nelken B, Reguerre Y, Bertrand Y, Haussinger D, Dalle JH, Ahmadian MR, Baruchel A, Chomienne C, Cave H. Juvenile myelomonocytic leukemia displays mutations in components of the RAS pathway and the PRC2 network. Nat Genet. 2015; 47:1334–1340. [PubMed: 26457648]

Chan G, Kalaitzidis D, Usenko T, Kutok JL, Yang W, Mohi MG, Neel BG. Leukemogenic Ptpn11 causes fatal myeloproliferative disorder via cell-autonomous effects on multiple stages of hema. Blood. 2009a; 113:4414–4424. [PubMed: 19179468]

Chan RJ, Cooper T, Kratz CP, Weiss B, Loh ML. Juvenile myelomonocytic leukemia: a report from the 2nd International JMML Symposium. Leuk Res. 2009b; 33:355–362. [PubMed: 18954903]

Chan RJ, Yoder MC. JMML patient-derived iPSCs induce new hypotheses. Blood. 2013; 121:4815–4817. [PubMed: 23766458]

Chen MJ, Li Y, De Obaldia ME, Yang Q, Yzaguirre AD, Yamada-Inagawa T, Vink CS, Bhandoola A, Dzierzak E, Speck NA. Erythroid/myeloid progenitors and hematopoietic stem cells originate from distinct populations of endothelial cells. Cell Stem Cell. 2011; 9:541–552. [PubMed: 22136929]

Christensen JL, Wright DE, Wagers AJ, Weissman IL. Circulation and chemotaxis of fetal hematopoietic stem cells. PLoS Biol. 2004; 2:E75. [PubMed: 15024423]

Cooper LJ, Shannon KM, Loken MR, Weaver M, Stephens K, Sievers EL. Evidence that juvenile myelomonocytic leukemia can arise from a pluripotential stem cell. Blood. 2000; 96:2310–2313. [PubMed: 10979983]

Croker B, Metcalf D, Robb L, Wei W, Mifsud S, DiRago L, Cluse L, Sutherland K, Hartley L, Williams E, Zhang JG, Hilton D, Nicola N, Alexander W. SOCS3 is a critical physiological negative regulator of G-CSF signaling and emergency granulopoiesis. Immunity. 2004; 20:153–165. [PubMed: 14975238]

de Boer J, Williams A, Skavdis G, Harker N, Coles M, Tolaini M, Norton T, Williams K, Roderick K, Potocnik AJ, Kioussis D. Transgenic mice with hematopoietic and lymphoid specific expression of Cre. European journal of immunology. 2003; 33:314–325. [PubMed: 12548562]

DeFalco T, Bhattacharya I, Williams AV, Sams DM, Capel B. Yolk-sac-derived macrophages regulate fetal testis vascularization and morphogenesis. Proc Natl Acad Sci U S A. 2014:E2384–E2393. [PubMed: 24912173]

Dong L, Yu WM, Zheng H, Loh ML, Bunting ST, Pauly M, Huang G, Zhou M, Broxmeyer HE, Scadden DT, Qu CK. Leukaemogenic effects of Ptpn11 activating mutations in the stem cell microenvironment. Nature. 2016; 539:304–308. [PubMed: 27783593]

Epelman S, Lavine KJ, Beaudin AE, Sojka DK, Carrero JA, Calderon B, Brija T, Gautier EL, Ivanov S, Satpathy AT, Schilling JD, Schwendener R, Sergin I, Razani B, Forsberg EC, Yokoyama WM, Unanue ER, Colonna M, Randolph GJ, Mann DL. Embryonic and adult-derived resident cardiac macrophages are maintained through distinct mechanisms at steady state and during inflammation. Immunity. 2014; 40:91–104. [PubMed: 24439267]

Espin-Palazon R, Stachura DL, Campbell CA, Garcia-Moreno D, Del Cid N, Kim AD, Candel S, Meseguer J, Mulero V, Traver D. Proinflammatory signaling regulates hematopoietic stem cell emergence. Cell. 2014; 159:1070–1085. [PubMed: 25416946]

Frame JM, Fegan KH, Conway SJ, McGrath KE, Palis J. Definitive Hematopoiesis in the Yolk Sac Emerges from Wnt-Responsive Hemogenic Endothelium Independently of Circulation and Arterial Identity. Stem Cells. 2016; 34:431–444. [PubMed: 26418893]

Frame JM, McGrath KE, Palis J. Erythro-myeloid progenitors: “definitive” hematopoiesis in the conceptus prior to the emergence of hematopoietic stem cells. Blood Cells Mol Dis. 2013; 51:220–225. [PubMed: 24095199]

Gandre-Babbe S, Paluru P, Aribeana C, Chou ST, Bresolin S, Lu L, Sullivan SK, Tasian SK, Weng J, Favre H, Choi JK, French DL, Loh ML, Weiss MJ. Patient-derived induced pluripotent stem cells recapitulate hematopoietic abnormalities of juvenile myelomonocytic leukemia. Blood. 2013; 121:4925–4929. [PubMed: 23620576]

Ghiaur G, Ferkowicz MJ, Milsom MD, Bailey JL, Witte D, Cancelas JA, Yoder MC, Williams DA. Rac1 is essential for intraembryonic hematopoiesis and for the initial seeding of fetal liver with definitive hem. Blood. 2008; 111:3313–3321. [PubMed: 18083846]

Ginhoux F, Greter M, Leboeuf M, Nandi S, See P, Gokhan S, Mehler MF, Conway SJ, Ng LG, Stanley ER, Samokhvalov IM, Merad M. Fate mapping analysis reveals that adult microglia derive from primitive macrophages. Science. 2010; 330:841–845. [PubMed: 20966214]

Gomez Perdiguero E, Klapproth K, Schulz C, Busch K, Azzoni E, Crozet L, Garner H, Trouillet C, de Bruijn MF, Geissmann F, Rodewald HR. Tissue-resident macrophages originate from yolk-sac-derived erythro-myeloid progenitors. Nature. 2015; 518:547–551. [PubMed: 25470051]

Gordon SR, Maute RL, Dulken BW, Hutter G, George BM, McCracken MN, Gupta R, Tsai JM, Sinha R, Corey D, Ring AM, Connolly AJ, Weissman IL. PD-1 expression by tumour-associated macrophages inhibits phagocytosis and tumour immunity. Nature. 2017; 545:495–499. [PubMed: 28514441]

Gosselin D, Link VM, Romanoski CE, Fonseca GJ, Eichenfield DZ, Spann NJ, Stender JD, Chun HB, Garner H, Geissmann F, Glass CK. Environment drives selection and function of enhancers controlling tissue-specific macrophage identities. Cell. 2014; 159:1327–1340. [PubMed: 25480297]

Haniffa M, Ginhoux F, Wang XN, Bigley V, Abel M, Dimmick I, Bullock S, Grisotto M, Booth T, Taub P, Hilkens C, Merad M, Collin M. Differential rates of replacement of human dermal dendritic cells and macrophages during hematopoietic stem cell transplantation. J Exp Med. 2009; 206:371–385. [PubMed: 19171766]

Hashimoto D, Chow A, Noizat C, Teo P, Beasley MB, Leboeuf M, Becker CD, See P, Price J, Lucas D, Greter M, Mortha A, Boyer SW, Forsberg EC, Tanaka M, van Rooijen N, Garcia-Sastre A, Stanley ER, Ginhoux F, Frenette PS, Merad M. Tissue-resident macrophages self-maintain locally throughout adult life with minimal contribution from circulating monocytes. Immunity. 2013; 38:792–804. [PubMed: 23601688]

Helsmoortel HH, Bresolin S, Lammens T, Cave H, Noellke P, Caye A, Ghazavi F, de Vries A, Hasle H, Labarque V, Masetti R, Stary J, van den Heuvel-Eibrink MM, Philippe J, Van Roy N, Benoit Y, Speleman F, Niemeyer C, Flotho C, Basso G, Te Kronnie G, Van Vlierberghe P, De Moerloose B. LIN28B overexpression defines a novel fetal-like subgroup of juvenile myelomonocytic leukemia. Blood. 2016; 127:1163–1172. [PubMed: 26712910]

Hoeffel G, Chen J, Lavin Y, Low D, Almeida FF, See P, Beaudin AE, Lum J, Low I, Forsberg EC, Poidinger M, Zolezzi F, Larbi A, Ng LG, Chan JK, Greter M, Becher B, Samokhvalov IM, Merad M, Ginhoux F. C-myb(+) erythro-myeloid progenitor-derived fetal monocytes give rise to adult tissue-resident macrophages. Immunity. 2015; 42:665–678. [PubMed: 25902481]

Kasaai B, Caolo V, Peacock HM, Lehoux S, Gomez-Perdiguero E, Luttun A, Jones EA. Erythro-myeloid progenitors can differentiate from endothelial cells and modulate embryonic vascular remodeling. Sci Rep. 2017; 7:43817. [PubMed: 28272478]

Kennedy DW, Abkowitz JL. Kinetics of central nervous system microglial and macrophage engraftment: analysis using a transgenic bone marrow transplantation model. Blood. 1997; 90:986–993. [PubMed: 9242527]

Kierdorf K, Erny D, Goldmann T, Sander V, Schulz C, Perdiguero EG, Wieghofer P, Heinrich A, Riemke P, Holscher C, Muller DN, Luckow B, Brocker T, Debowski K, Fritz G, Opdenakker G, Diefenbach A, Biber K, Heikenwalder M, Geissmann F, Rosenbauer F, Prinz M. Microglia emerge from erythromyeloid precursors via Pu.1- and Irf8-dependent pathways. Nat Neurosci. 2013; 16:273–280. [PubMed: 23334579]

Kratz CP, Niemeyer CM, Castleberry RP, Cetin M, Bergstrasser E, Emanuel PD, Hasle H, Kardos G, Klein C, Kojima S, Stary J, Trebo M, Zecca M, Gelb BD, Tartaglia M, Loh ML. The mutational

spectrum of PTPN11 in juvenile myelomonocytic leukemia and Noonan syndrome/myeloproliferative disease. Blood. 2005; 106:2183–2185. [PubMed: 15928039]

Lavin Y, Winter D, Blecher-Gonen R, David E, Keren-Shaul H, Merad M, Jung S, Amit I. Tissue-resident macrophage enhancer landscapes are shaped by the local microenvironment. Cell. 2014; 159:1312–1326. [PubMed: 25480296]

Li Y, Esain V, Teng L, Xu J, Kwan W, Frost IM, Yzaguirre AD, Cai X, Cortes M, Maijenburg MW, Tober J, Dzierzak E, Orkin SH, Tan K, North TE, Speck NA. Inflammatory signaling regulates embryonic hematopoietic stem and progenitor cell production. Genes Dev. 2014; 28:2597–2612. [PubMed: 25395663]

Li Z, Godinho FJ, Klusmann JH, Garriga-Canut M, Yu C, Orkin SH. Developmental stage-selective effect of somatically mutated leukemogenic transcription factor GATA1. Nat Genet. 2005; 37:613–619. [PubMed: 15895080]

Lin Y, Yoder MC, Yoshimoto M. Lymphoid progenitor emergence in the murine embryo and yolk sac precedes stem cell detection. Stem Cells Dev. 2014; 23:1168–1177. [PubMed: 24417306]

Liu X, Zheng H, Li X, Wang S, Meyerson HJ, Yang W, Neel BG, Qu CK. Gain-of-function mutations of Ptpn11 (Shp2) cause aberrant mitosis and increase susceptibility to DNA damage-induced malignancies. Proc Natl Acad Sci U S A. 2016; 113:984–989. [PubMed: 26755576]

Locatelli F, Crotta A, Ruggeri A, Eapen M. Analysis of risk factors influencing outcomes after cord blood transplantation in children with juvenile myelomonocytic leukemia: a EUROCORD, EBMT, EWOG. Blood. 2013; 122:2135–2141. [PubMed: 23926304]

Locatelli F, Niemeyer CM. How I treat juvenile myelomonocytic leukemia. Blood. 2015; 125:1083–1090. [PubMed: 25564399]

Locatelli F, Nöllke P, Zecca M, Korthof E, Lanino E, Peters C, Pession A, Kabisch H, Uderzo C, Bonfim CS, Bader P, Dilloo D, Stary J, Fischer A, Révész T, Führer M, Hasle H, Trebo M, van den Heuvel-Eibrink MM, Fenu S, Strahm B, Giorgiani G, Bonora MR, Duffner U, Niemeyer CM. Hematopoietic stem cell transplantation (HSCT) in children with juvenile myelomonocytic leukemia (JMML): results of the EWOG-MDS/EBMT trial. Blood. 2005; 105:410–419. [PubMed: 15353481]

Lux CT, Yoshimoto M, McGrath KE, Conway SJ, Palis J, Yoder MC. All primitive and definitive hematopoietic progenitor cells emerging before E10 in the mouse embryo are products of the yolk sac. Blood. 2008; 111:3435–3438. [PubMed: 17932251]

Matsuda K, Sakashita K, Taira C, Tanaka-Yanagisawa M, Yanagisawa R, Shiohara M, Kanegane H, Hasegawa D, Kawasaki K, Endo M, Yajima S, Sasaki S, Kato K, Koike K, Kikuchi A, Ogawa A, Watanabe A, Sotomatsu M, Nonoyama S. Quantitative assessment of PTPN11 or RAS mutations at the neonatal period and during the clinical course in patients with juvenile myelomonocytic leukaemia. Br J Haematol. 2010; 148:593–599. [PubMed: 19874312]

McGrath KE, Frame JM, Fegan KH, Bowen JR, Conway SJ, Catherman SC, Kingsley PD, Koniski AD, Palis J. Distinct Sources of Hematopoietic Progenitors Emerge before HSCs and Provide Functional Blood Cells in the Mammalian Embryo. Cell Rep. 2015; 11:1892–1904. [PubMed: 26095363]

Moore MA, Metcalf D. Ontogeny of the Haemopoietic System Yolk Sac Origin of In Viuo and In Vitro Colony Forming Cells in the Developing Mouse Embryo. Br J Haematol. 1969; 18:279–296.

Mucenski ML, McLain K, Kier AB, Swerdlow SH, Schreiner CM, Miller TA, Pietryga DW, Scott WJJ, Potter SS. A functional c-myb gene is required for normal murine fetal hepatic hematopoiesis. Cell. 1991; 65:677–689. [PubMed: 1709592]

Mulero-Navarro S, Sevilla A, Roman AC, Lee DF, D'Souza SL, Pardo S, Riess I, Su J, Cohen N, Schaniel C, Rodriguez NA, Baccarini A, Brown BD, Cave H, Caye A, Strullu M, Yalcin S, Park CY, Dhandapany PS, Yongchao G, Edelmann L, Bahieg S, Raynal P, Flex E, Tartaglia M, Moore KA, Lemischka IR, Gelb BD. Myeloid Dysregulation in a Human Induced Pluripotent Stem Cell Model of PTPN11-Associated Juvenile Myelomonocytic Leukemia. Cell Rep. 2015; 13:504–515. [PubMed: 26456833]

Muller AM, Medvinsky A, Strouboulis J, Grosveld F, Dzierzak E. Development of Hematopoietic in the Mouse Embryo Stem Cell Activity. Immunity. 1994; 1:291–301. [PubMed: 7889417]

Olk-Batz C, Poetsch AR, Nollke P, Claus R, Zucknick M, Sandrock I, Witte T, Strahm B, Hasle H, Zecca M, Stary J, Bergstraesser E, De Moerloose B, Trebo M, van den Heuvel-Eibrink MM, Wojcik D, Locatelli F, Plass C, Niemeyer CM, Flotho C. European Working Group of Myelodysplastic Syndromes in C. Aberrant DNA methylation characterizes juvenile myelomonocytic leukemia with poor outcome. Blood. 2011; 117:4871–4880. [PubMed: 21406719]

Palis J, Robertson S, Kennedy M, Wall C, Keller G. Development of erythroid and myeloid progenitors in the yolk sac and embryo proper of the mouse.pdf. Development. 1999; 126:5073–5084. [PubMed: 10529424]

Qian BZ, Li J, Zhang H, Kitamura T, Zhang J, Campion LR, Kaiser EA, Snyder LA, Pollard JW. CCL2 recruits inflammatory monocytes to facilitate breast-tumour metastasis. Nature. 2011; 475:222–225. [PubMed: 21654748]

Rybtsov S, Sobiesiak M, Taoudi S, Souilhol C, Senserrich J, Liakhovitskaia A, Ivanovs A, Frampton J, Zhao S, Medvinsky A. Hierarchical organization and early hematopoietic specification of the developing HSC lineage in the AGM region. J Exp Med. 2011; 208:1305–1315. [PubMed: 21624936]

Sakaguchi H, Okuno Y, Muramatsu H, Yoshida K, Shiraishi Y, Takahashi M, Kon A, Sanada M, Chiba K, Tanaka H, Makishima H, Wang X, Xu Y, Doisaki S, Hama A, Nakanishi K, Takahashi Y, Yoshida N, Maciejewski JP, Miyano S, Ogawa S, Kojima S. Exome sequencing identifies secondary mutations of SETBP1 and JAK3 in juvenile myelomonocytic leukemia. Nat Genet. 2013; 45:937–941. [PubMed: 23832011]

Samokhvalov IM, Samokhvalova NI, Nishikawa S. Cell tracing shows the contribution of the yolk sac to adult haematopoiesis. Nature. 2007; 446:1056–1061. [PubMed: 17377529]

Schlenner SM, Rodewald HR. Early T cell development and the pitfalls of potential. Trends Immunol. 2010; 31:303–310. [PubMed: 20634137]

Schulz C, Gomez Perdiguero E, Chorro L, Szabo-Rogers H, Cagnard N, Kierdorf K, Prinz M, Wu B, Jacobsen SE, Pollard JW, Frampton J, Liu KJ, Geissmann F. A lineage of myeloid cells independent of Myb and hematopoietic stem cells. Science. 2012; 336:86–90. [PubMed: 22442384]

Sheng J, Ruedl C, Karjalainen K. Fetal HSCs versus EMP2s. Immunity. 2015; 43:1025. [PubMed: 26682974]

Stadtfeld M, Ye M, Graf T. Identification of interventricular septum precursor cells in the mouse embryo. Dev Biol. 2007; 302:195–207. [PubMed: 17064678]

Stieglitz E, Taylor-Weiner AN, Chang TY, Gelston LC, Wang YD, Mazor T, Esquivel E, Yu A, Seepo S, Olsen SR, Rosenberg M, Archambeault SL, Abusin G, Beckman K, Brown PA, Briones M, Carcamo B, Cooper T, Dahl GV, Emanuel PD, Fluchel MN, Goyal RK, Hayashi RJ, Hitzler J, Hugge C, Liu YL, Messinger YH, Mahoney DH Jr, Monteleone P, Nemecek ER, Roehrs PA, Schore RJ, Stine KC, Takemoto CM, Toretsky JA, Costello JF, Olshen AB, Stewart C, Li Y, Ma J, Gerbing RB, Alonzo TA, Getz G, Gruber TA, Golub TR, Stegmaier K, Loh ML. The genomic landscape of juvenile myelomonocytic leukemia. Nat Genet. 2015; 47:1326–1333. [PubMed: 26457647]

Tanaka Y, Hayashi M, Kubota Y, Nagai H, Sheng G, Nishikawa S, Samokhvalov IM. Early ontogenic origin of the hematopoietic stem cell lineage. Proc Natl Acad Sci U S A. 2012; 109:4515–4520. [PubMed: 22392989]

Tober J, Koniski A, McGrath KE, Vemishetti R, Emerson R, de Mesy-Bentley KK, Waugh R, Palis J. The megakaryocyte lineage originates from hemangioblast precursors and is an integral component both of primitive and of definitive hematopoiesis. Blood. 2007; 109:1433–1441. [PubMed: 17062726]

Tober J, Yzaguirre AD, Piwarzyk E, Speck NA. Distinct temporal requirements for Runx1 in hematopoietic progenitors and stem cells. Development. 2013; 140:3765–3776. [PubMed: 23924635]

Vanhee S, De Mulder K, Van Caeneghem Y, Verstichel G, Van Roy N, Menten B, Velghe I, Philippe J, De Bleser D, Lambrecht BN, Taghon T, Leclercq G, Kerre T, Vandekerckhove B. In vitro human embryonic stem cell hematopoiesis mimics MYB-independent yolk sac hematopoiesis. Haematologica. 2015; 100:157–166. [PubMed: 25381126]

Weinberg RS, Leibowitz D, Weinblatt ME, Kochen J, Alter BP. Juvenile chronic myelogenous leukaemia: the only example of truly fetal (not fetal-like) erythropoiesis. Br J Haematol. 1990; 76:307–310. [PubMed: 1709807]

Xu D, Liu X, Yu WM, Meyerson HJ, Guo C, Gerson SL, Qu CK. Non-lineage/stage-restricted effects of a gain-of-function mutation in tyrosine phosphatase Ptpn11 (Shp2) on malignant transformation of hematopoietic cells. J Exp Med. 2011; 208:1977–1988. [PubMed: 21930766]

Xu D, Zheng H, Yu WM, Qu CK. Activating mutations in protein tyrosine phosphatase Ptpn11 (Shp2) enhance reactive oxygen species production that contributes to myeloproliferative disorder. PLoS One. 2013; 8:e63152. [PubMed: 23675459]

Yoder MC, Hiatt K. Engraftment of Embryonic Hematopoietic Cells in Conditioned Newborn Recipients. Blood. 1997; 89:2176–2183. [PubMed: 9058742]

Yoder MC, Hiatt K, Dutt P, Mukherjee P, Bodine DM, Orlic D. Characterization of definitive lymphohematopoietic stem cells in the day 9 murine yolk sac. Immunity. 1997; 7:335–344. [PubMed: 9324354]

Yoshimoto M, Montecino-Rodriguez E, Ferkowicz MJ, Porayette P, Shelley WC, Conway SJ, Dorshkind K, Yoder MC. Embryonic day 9 yolk sac and intra-embryonic hemogenic endothelium independently generate a B-1 and marginal zone progenitor lacking B-2 potential. Proc Natl Acad Sci U S A. 2010; 108:1468–1473.

Yoshimoto M, Porayette P, Glosson NL, Conway SJ, Carlesso N, Cardoso AA, Kaplan MH, Yoder MC. Autonomous murine T-cell progenitor production in the extra-embryonic yolk sac before HSC emergence. Blood. 2012; 119:5706–5714. [PubMed: 22431573]

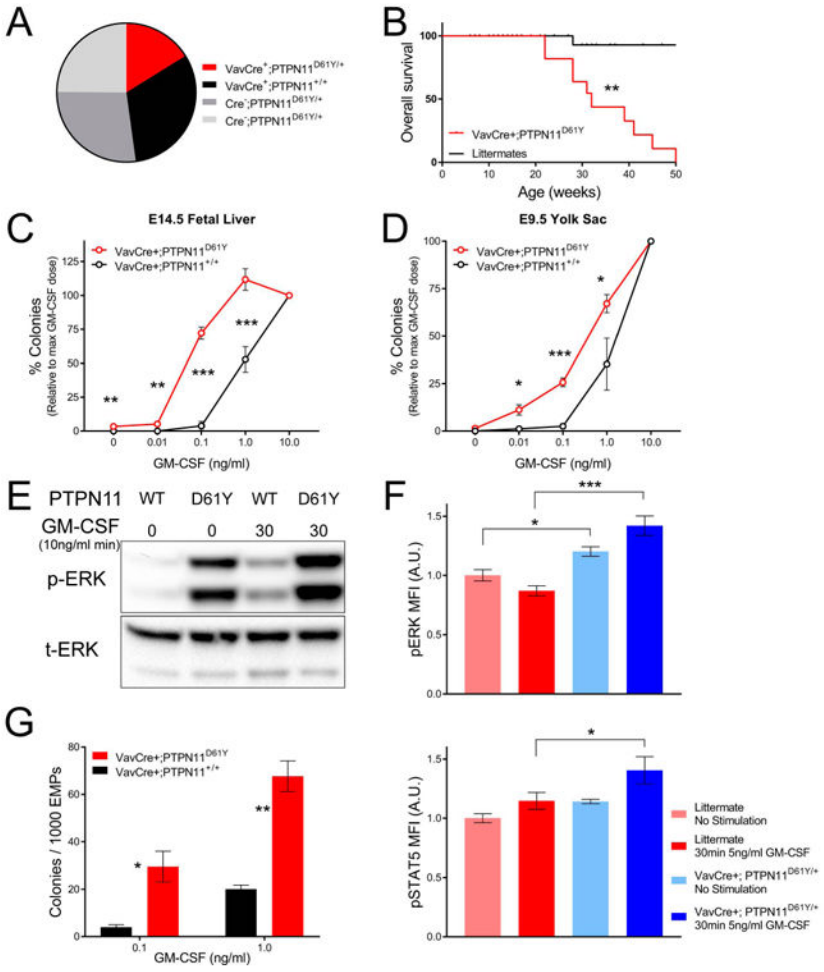


**Figure 1. VavCre+;PTPN11$^{D61Y}$ E9.5 yolk sac EMPs have defining features of JMML**

A) Genotype ratios at weaning of VavCre+ × PTPN11$^{D61Y/+}$ matings; Chi-Squared p-value=0.04. B) Overall survival of VavCre+ × PTPN11$^{D61Y/+}$ progeny (N=12 mutants, 53 littermates). C,D) 7 day methylcellulose colony formation of E14.5 FL cells (N=7 mutants, 7 controls) and E9.5 YS cells (N=11 mutants, 7 controls). E) *Ex vivo* FL-derived macrophages were stimulated for 30min with 10ng/ml GM-CSF and lysates were probed with indicated antibodies. F) p-ERK and p-STAT5 signaling in *ex vivo* cultures of E9.5 YS-derived macrophages following 30min of 5ng/ml GM-CSF stimulation (N=5 biological replicates/ group from 2 independent experiments). G) Methylcellulose assay with E9.5 YS sorted Ter119- cKit+ CD41$^{dim}$ EMPs (N=2 pooled litters).

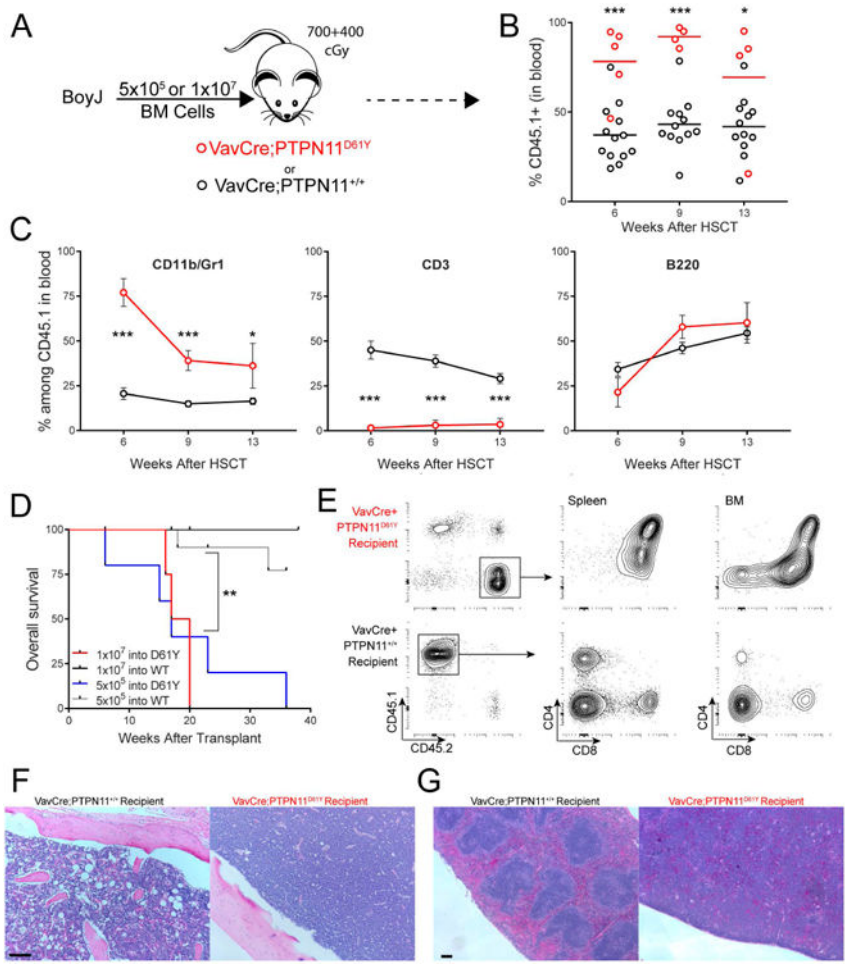


**Figure 2. VavCre+;PTPN11$^{D61Y}$ acquire T-ALL following healthy donor HSCT**

A) Schematic of transplant. B) Donor engraftment in blood. C) Donor contribution to myeloid and lymphoid peripheral blood leukocytes. D) Overall survival of transplant recipients. E) Representative flow cytometry of CD45.2+ host-derived abnormal T-lymphocytes in the BM and spleen of mutant recipients. Immunohistochemistry of F) BM and G) spleen of mutant and littermate transplant recipients.

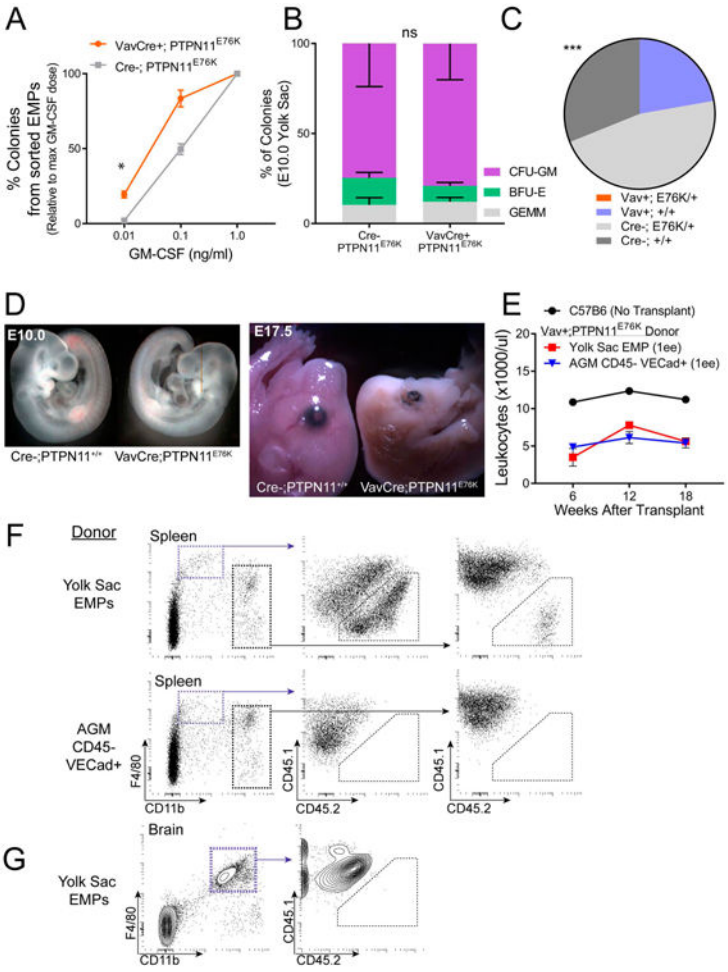


**Figure 3. VavCre+;PTPN11$^{E76K}$ YS EMPs engraft neonatal recipients but do not give rise to MPN**

A) 7 day colony formation from sorted Ter119- cKit+ CD41$^{dim}$ E10.0 YS EMPs (n=4 embryos/group from 2 litters). B) Methylcellulose colony formation by mutant and littermate YS progenitors (N=3 litters, analysis by Chi-Squared test). C) Genotype ratio of animals weaned from VavCre+ × PTPN11$^{E76K/+}$ matings (N=45 births). D) Representative images of E10.0 and E17.5 mutant and littermate embryos. E-G) YS and AGM progenitors from E10.5 VavCre+;PTPN11$^{E76K}$ embryos were transplanted into 2 day-old NSG neonatal recipients. E) Leukocyte counts of recipients (N=2 recipients/group). F) Representative gating of YS EMP-derived splenic macrophages in neonatal recipients. G) YS EMPs from mutant embryos do not contribute to microglial populations in engrafted animals.

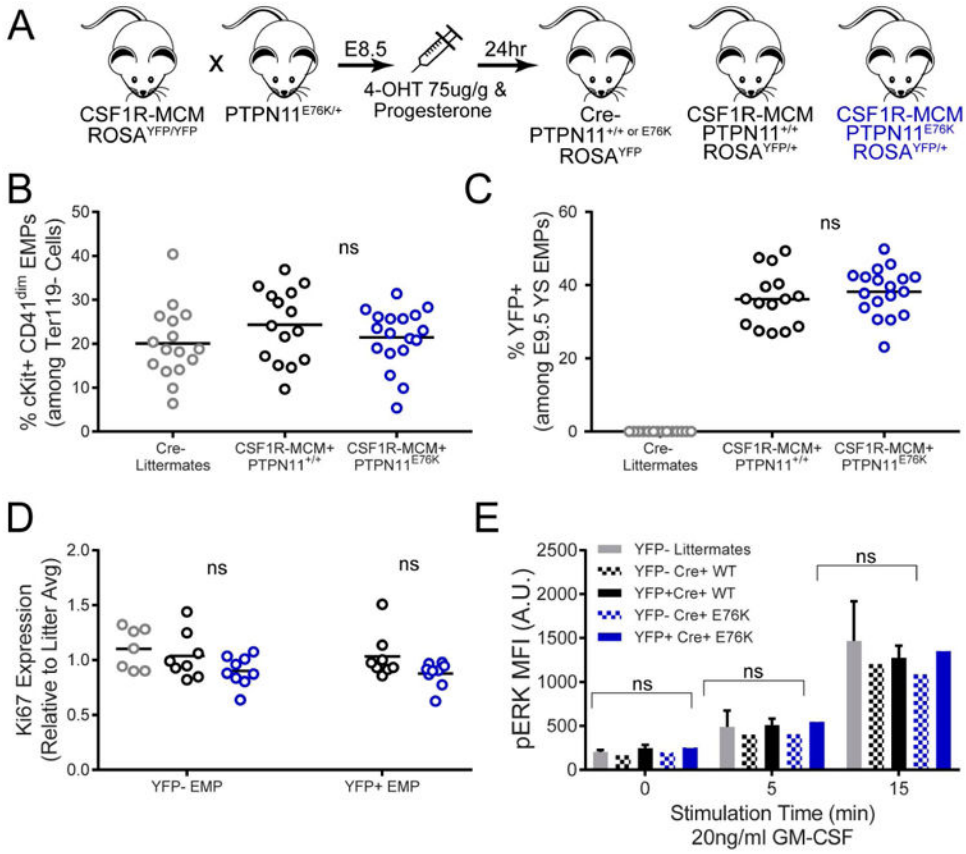


**Figure 4. Analysis of CSF1R-MCM+;ROSA$^{YFP}$;PTPN11$^{E76K}$ E9.5 EMPs**

A) Schematic of mating strategy and 4-hyroxy tamoxifen (4OHT) administration to pregnant dams. B) Frequency of EMPs in E9.5 YS. C) Proportion of EMPs that are YFP+ following E8.5 4OHT. D) Ki67 expression in E9.5 YS EMPs (normalized to average median fluorescence intensity among EMPs in each litter). E) p-ERK expression among *ex vivo* E9.5 YS EMP-derived macrophages after stimulation with 20ng/ml (N=3 embryos/group).

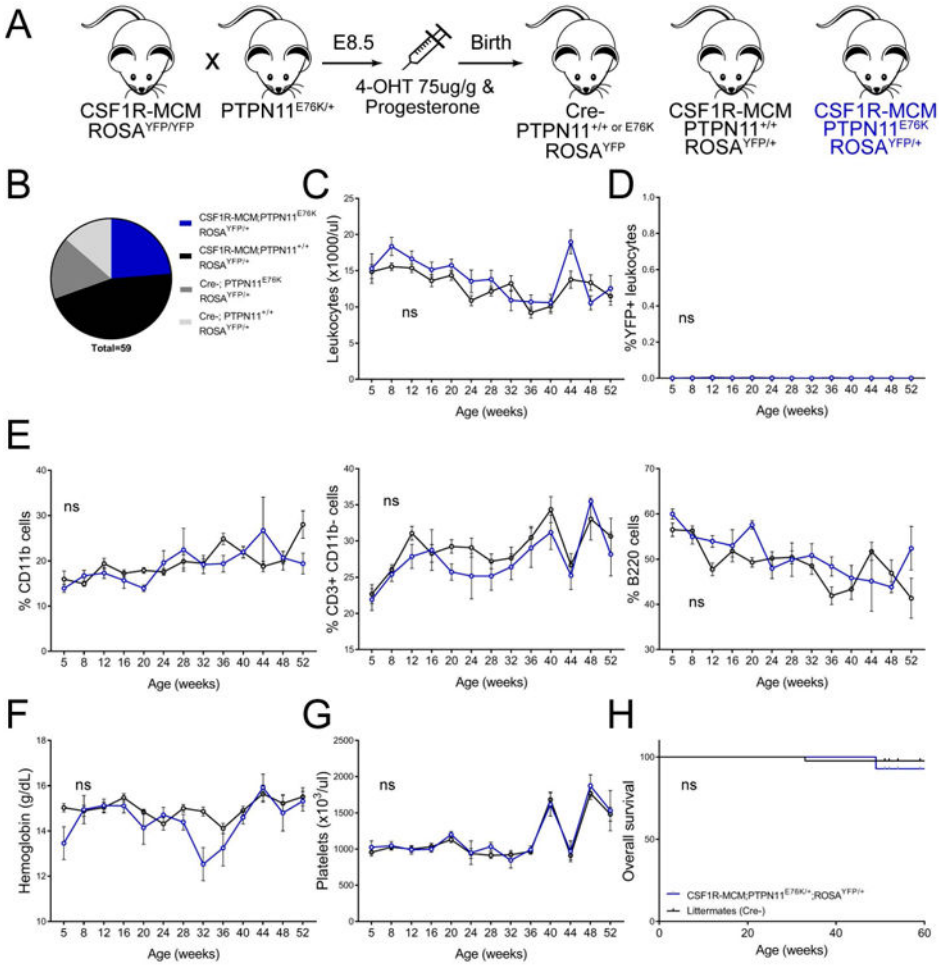


**Figure 5. Peripheral blood analysis of CSF1R-MCM+;ROSA$^{YFP}$;PTPN11$^{E76K}$**

A) Schematic of mating. All litters were born to dams who were injected with 4OHT at E8.5. B) Genotype ratios at weaning (N=14 mutants and 43 controls). C) CBC analysis of leukocyte frequency. D) Frequency of YFP+ leukocytes in peripheral blood. E) Frequency of myeloid and lymphoid progeny in peripheral blood. F,G) Hemoglobin and platelet abundance in peripheral blood). H) Overall survival.

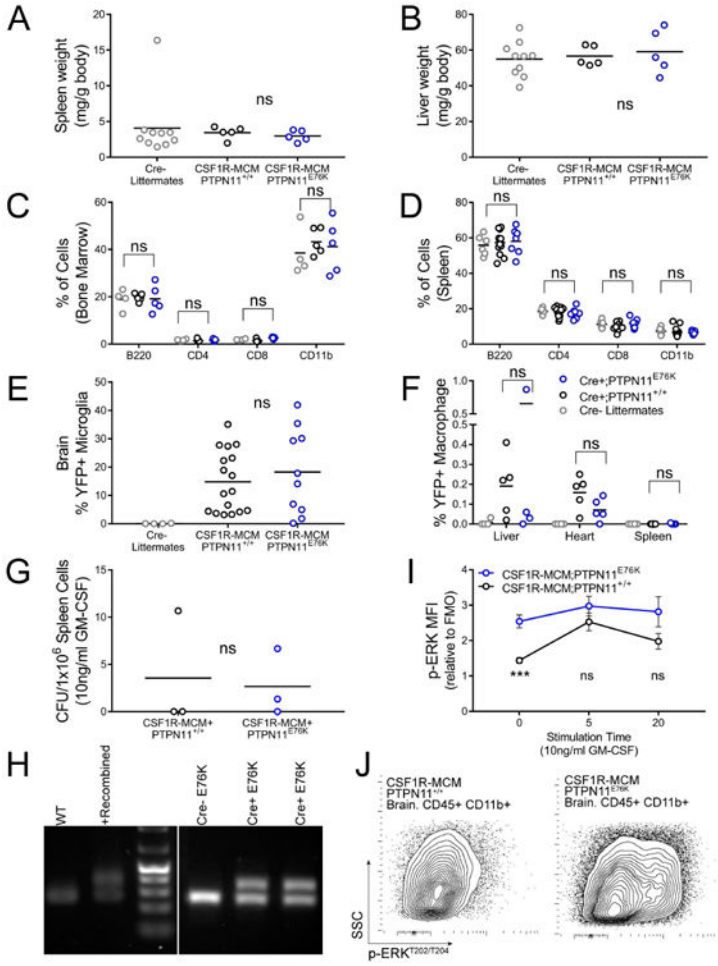


**Figure 6. Macrophage analysis in CSF1R-MCM+;ROSA$^{YFP}$;PTPN11$^{E76K}$ animals**

Analyses were performed 52-60 weeks after birth following *in utero* exposure to 4OHT at E8.5. A,B) Normalized weights of spleens and livers. C,D) Frequency of B-cells, T-cells, and myeloid cells in the bone marrow and spleen of mutants and littermates as measured by flow cytometry. E,F) Frequency of YFP+ macrophages (CD45+ CD11b+ F4/80+). G) 7 day methylcellulose colony formation from splenic progenitors cultured in in 10ng/ml GM-CSF. H) PCR analysis detects recombined LSL-PTPN11$^{E76K}$ locus in genomic DNA from mutant brain samples. Image is a concatenation of lanes run on a single gel. I) p-ERK expression in microglia following stimulation with 10ng/ml GM-CSF for indicated durations. (N=5 mutant and 12 controls). J) Representative p-ERK expression in freshly-harvested, unstimulated microglia.